

# Star Formation News Letter

## No. 275 #46-50

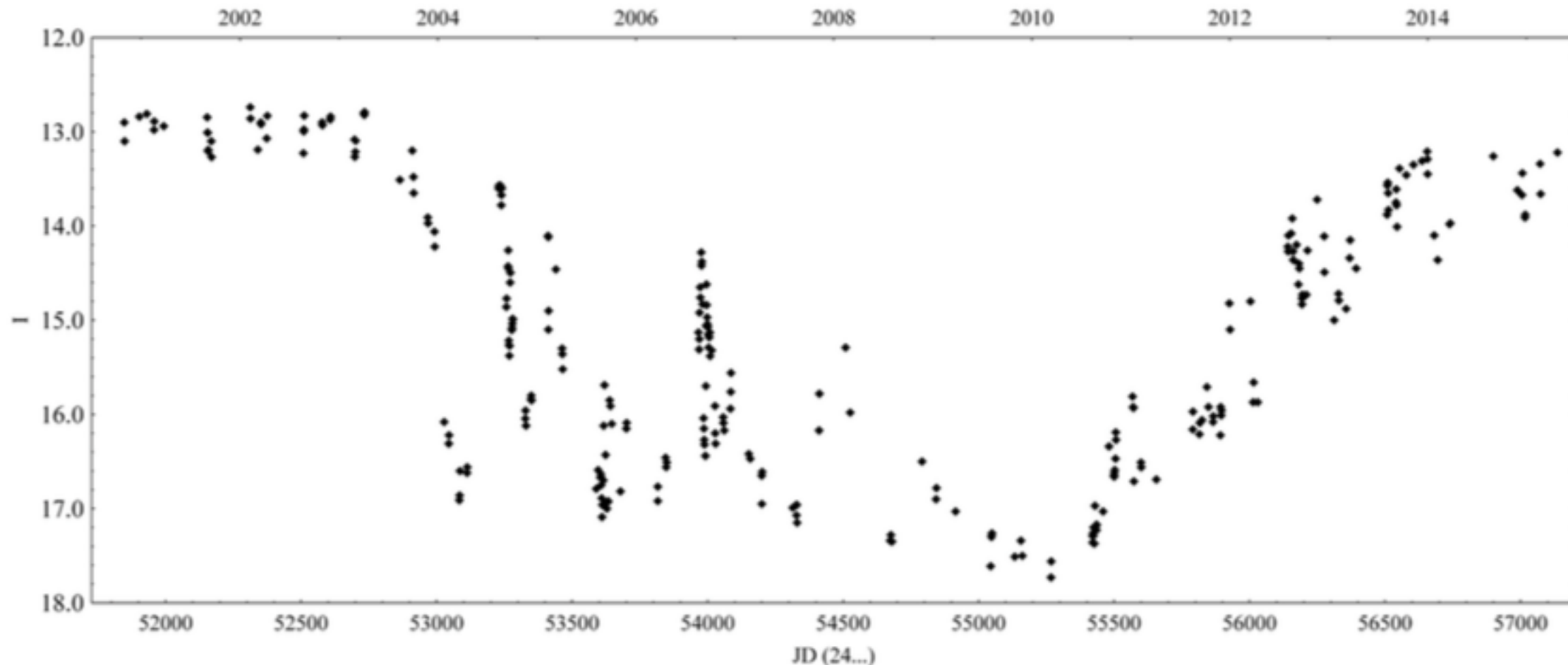
1. The PMS star V1184 Tau (CB 34V) at the end of prolonged eclipse, Semkov *et al.* A&A
2. Wobbling and precessing jets from warped disks in binary systems, Sheikhnezami *et al.* ApJ
3. Spectral-Line Survey at Millimeter and Submillimeter Wavelengths toward an Outflow- Shocked Region, OMC 2-FIR 4, Shimajiri *et al.* ApJS
4. Resolved Millimeter-Wavelength Observations of Debris Disks around Solar-Type Stars, Steele *et al.* ApJ
5. Dispersing Envelope around the Keplerian Circumbinary Disk in L1551 NE and its Implications for the Binary Growth, Takakuwa *et al.* ApJ

花輪 知幸

# The PMS star V1184 Tau (CB 34V) at the end of prolonged eclipse (Research Note)

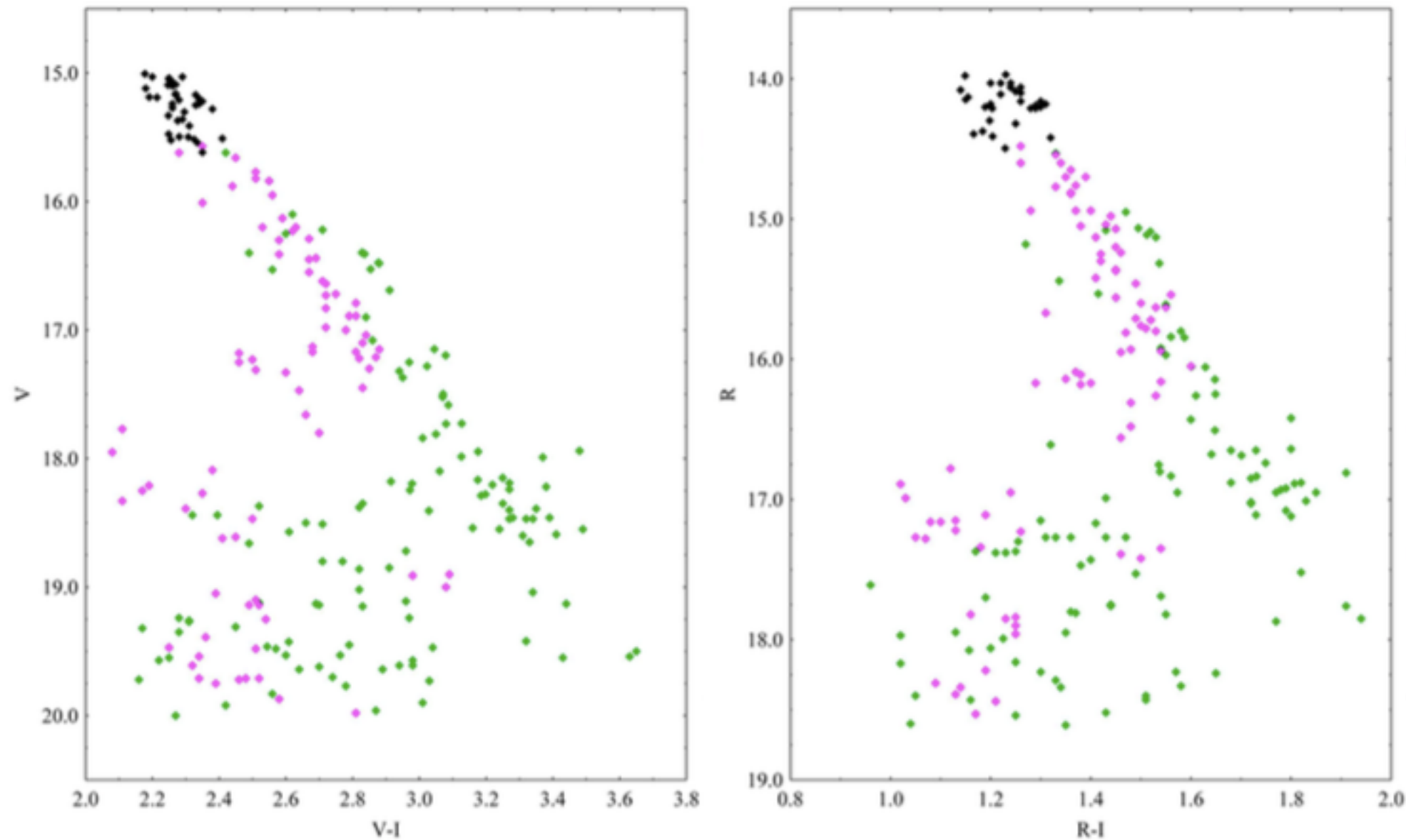
E. H. Semkov et al. A&A

CB34 = Bok globule



最も明るい時は典型的な T Tau  
4等の減光 Circumstellar

## 二つの二色図



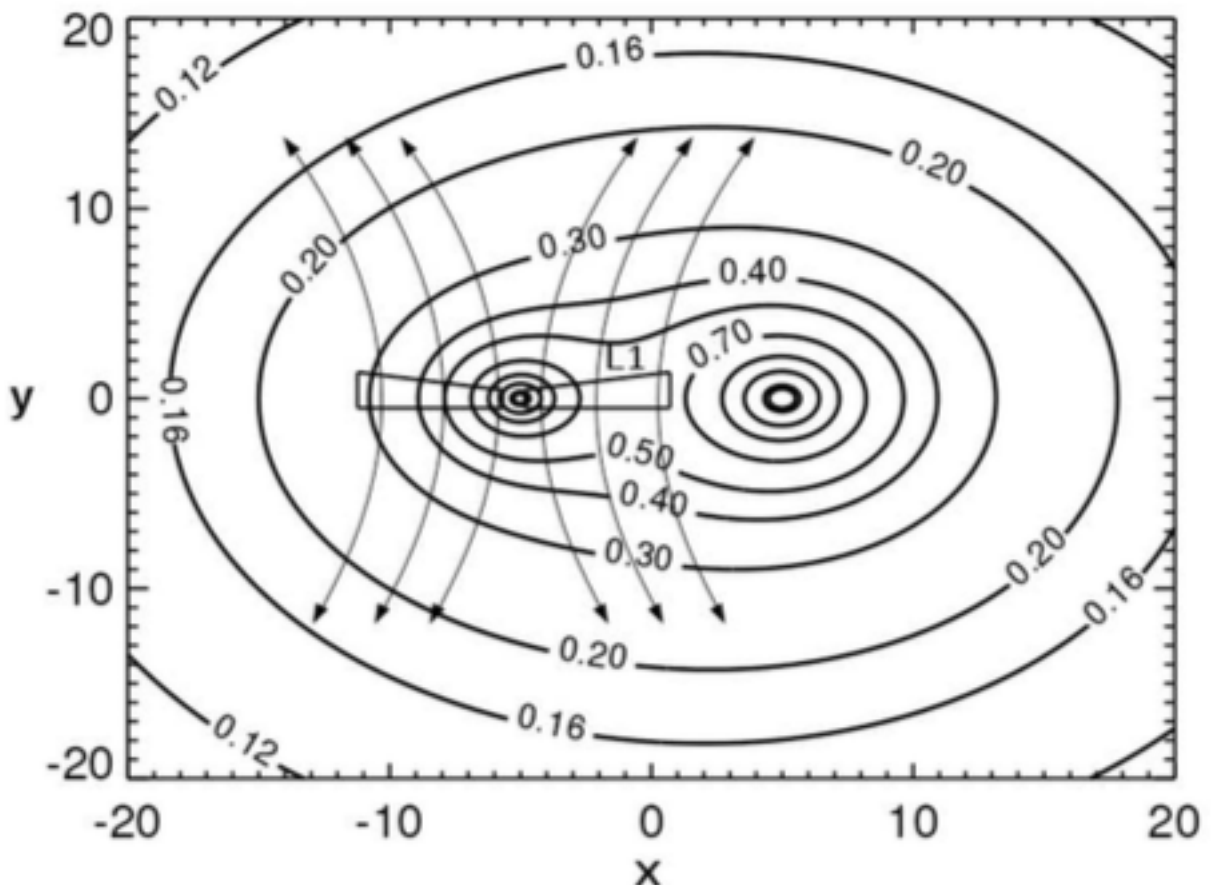
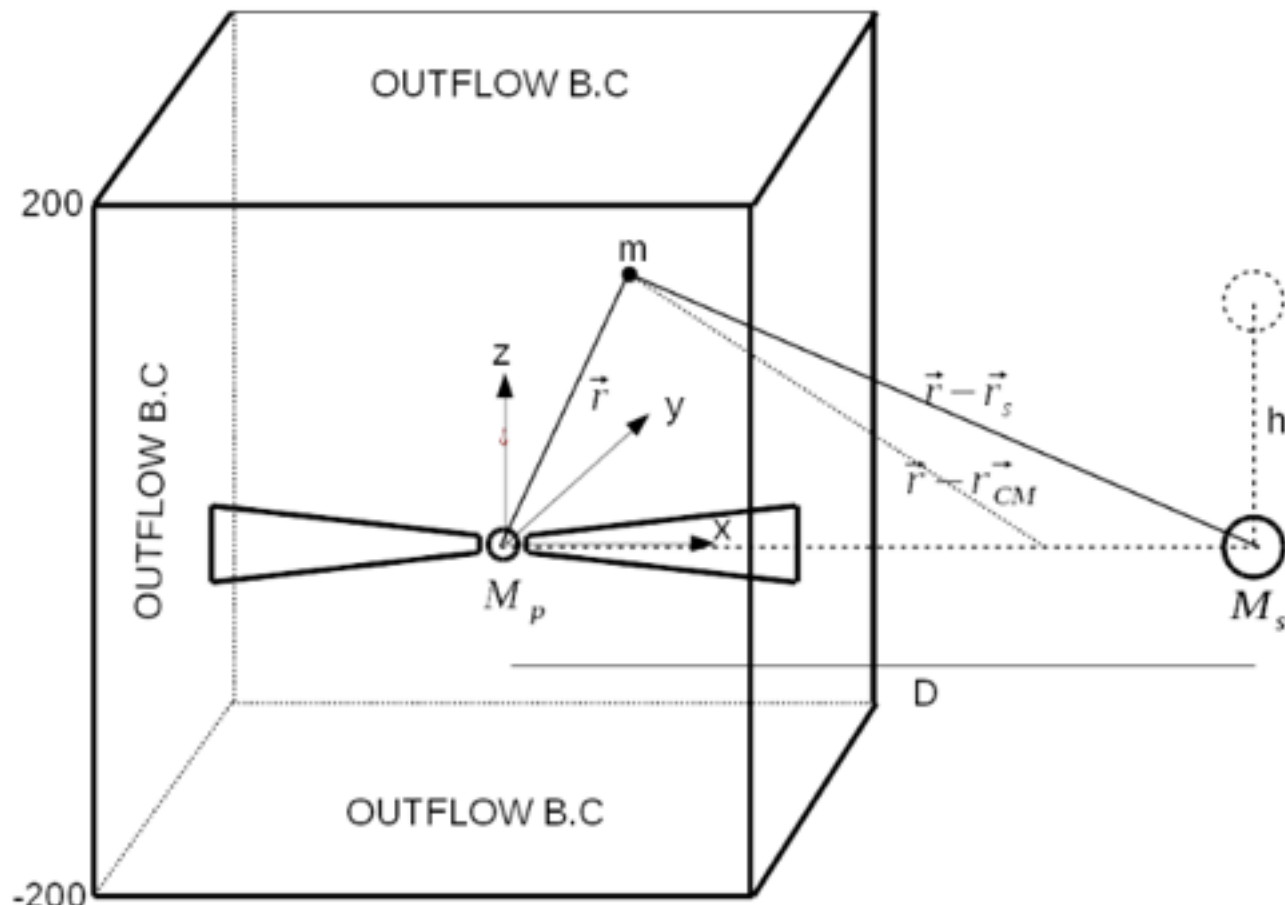
黒: 最大光度 緑 減光時 ピンク 増光時

青くなるのは散乱が増えるため

# WOBBLING AND PRECESSING JETS FROM WARPED DISKS IN BINARY SYSTEMS

Somayeh Sheikhnezami & Christian Fendt ApJ

3D MHD jets in Roche potential



Pluto, resistive inviscid MHD

Ohmic dissipation による加熱はすぐに放射されると近似

$$\frac{\partial \rho}{\partial t} + \nabla \cdot (\rho \vec{v}) = 0, \quad (1)$$

$$\frac{\partial(\rho \vec{v})}{\partial t} + \nabla \cdot \left( \vec{v} \rho \vec{v} - \frac{\vec{B} \vec{B}}{4\pi} \right) + \nabla \left( P + \frac{B^2}{8\pi} \right) + \rho \nabla \Phi = 0, \quad (2)$$

$$\begin{aligned} \frac{\partial e}{\partial t} + \nabla \cdot \left[ \left( e + P + \frac{B^2}{8\pi} \right) \vec{v} - (\vec{v} \cdot \vec{B}) \frac{\vec{B}}{4\pi} + (\eta \vec{j}) \times \frac{\vec{B}}{4\pi} \right] \\ = -\Lambda_{\text{cool}}. \end{aligned} \quad (3)$$

Ohmic dissipation による加熱はすぐ  
ぐに放射されると近似,  $\Lambda = \Gamma$

初期状態

$$\rho_d = \rho_{d,i} \left( \frac{2}{5\epsilon^2} \left[ \frac{r_i}{R} - \left( 1 - \frac{5\epsilon^2}{2} \right) \frac{r_i}{r} \right] \right)^{3/2}, \quad (6)$$

while for the initial disk pressure distribution we apply

$$P_d = P_{d,i} \left( \frac{\rho_{d,i}}{\rho_d} \right)^{5/3}. \quad (7)$$

初期磁場 (flux function,  $A_\phi$ )

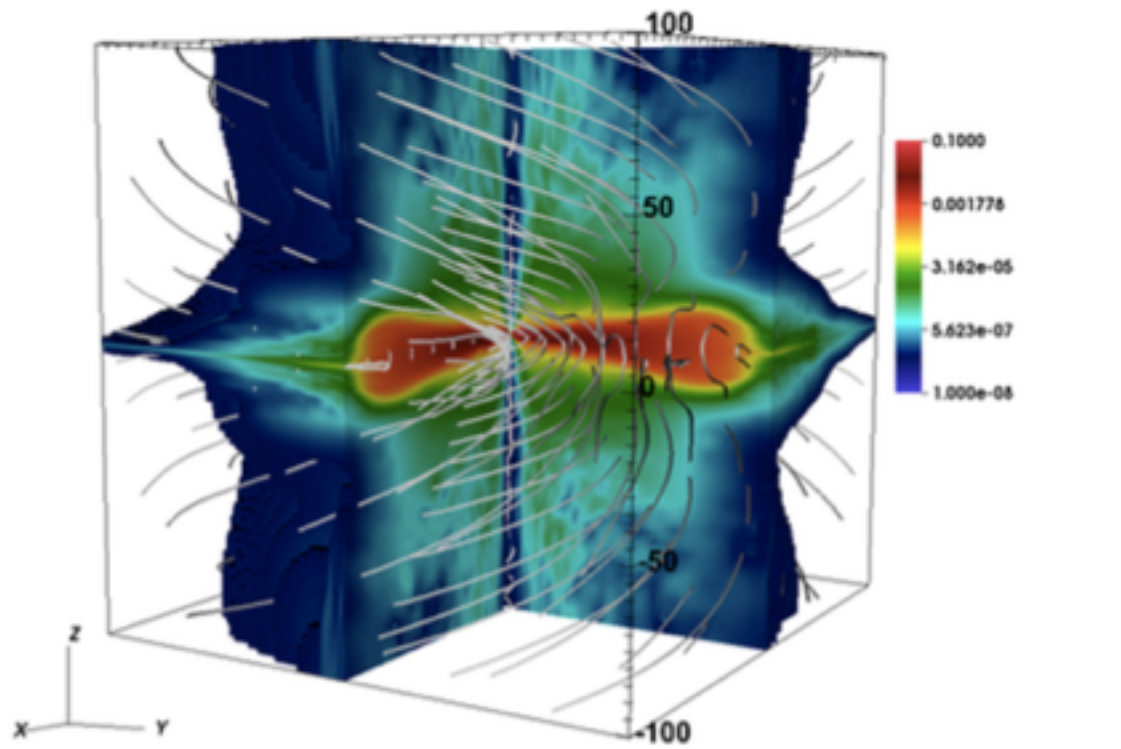
$$\psi(x, y, z) = 3/4 B_{z,i} r_i^2 \left( \frac{r}{r_i} \right)^{3/4} \frac{m^{5/4}}{(m^2 + (z/r)^2)^{5/8}}, \quad (8)$$

## 单独星と連星

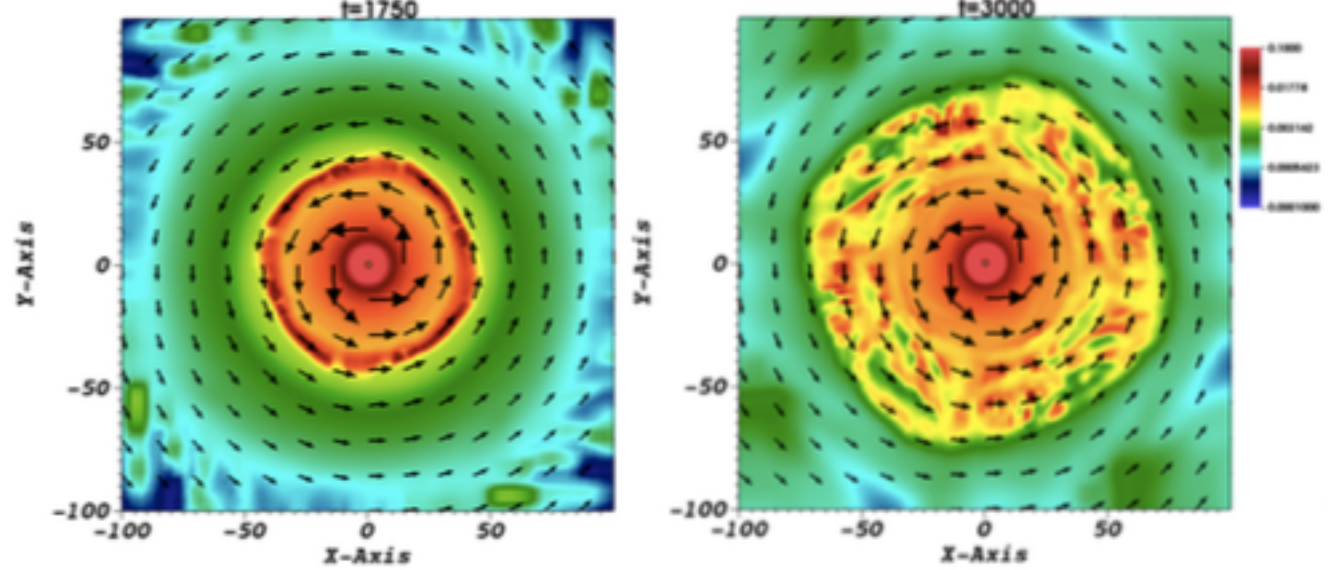
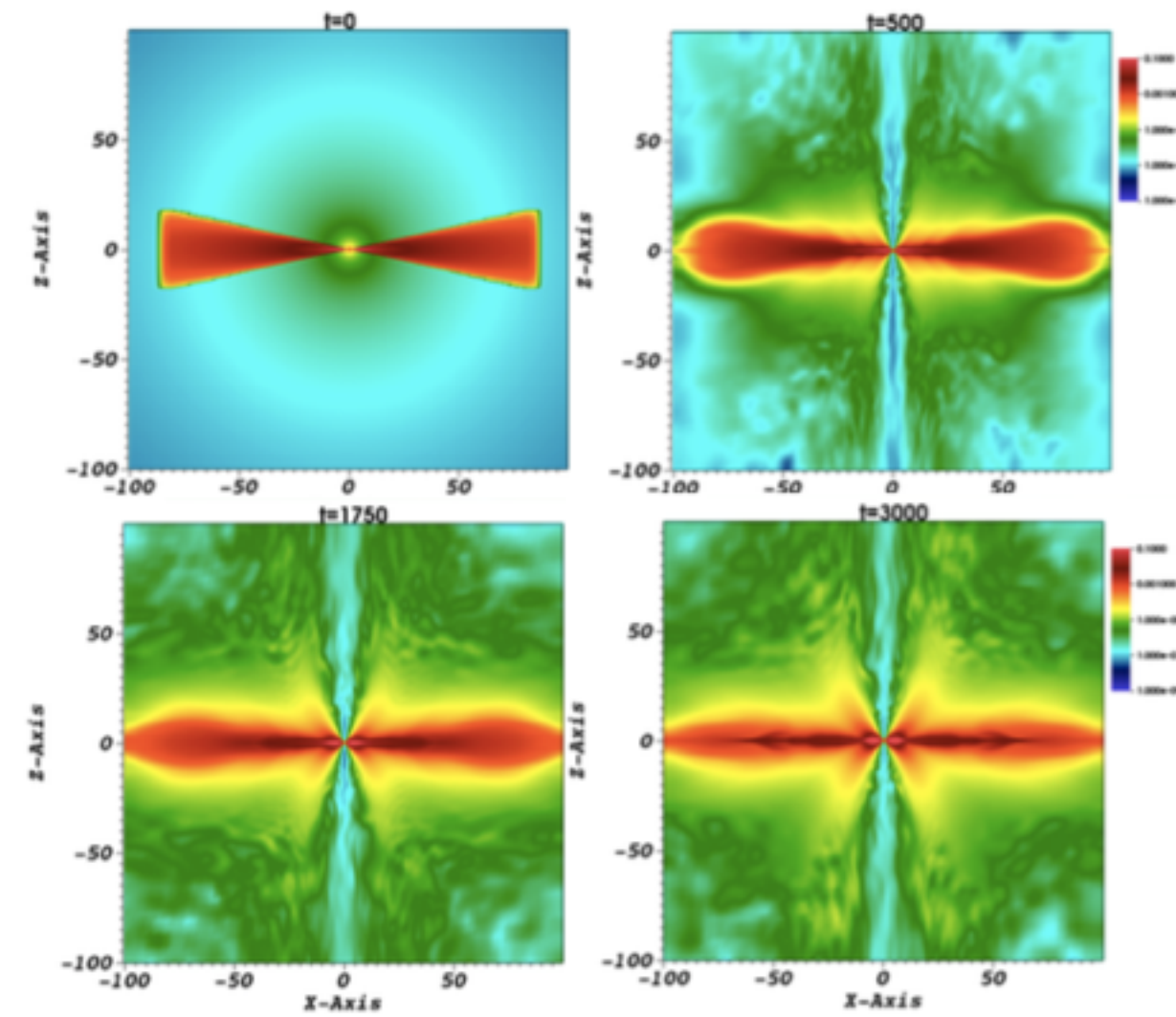
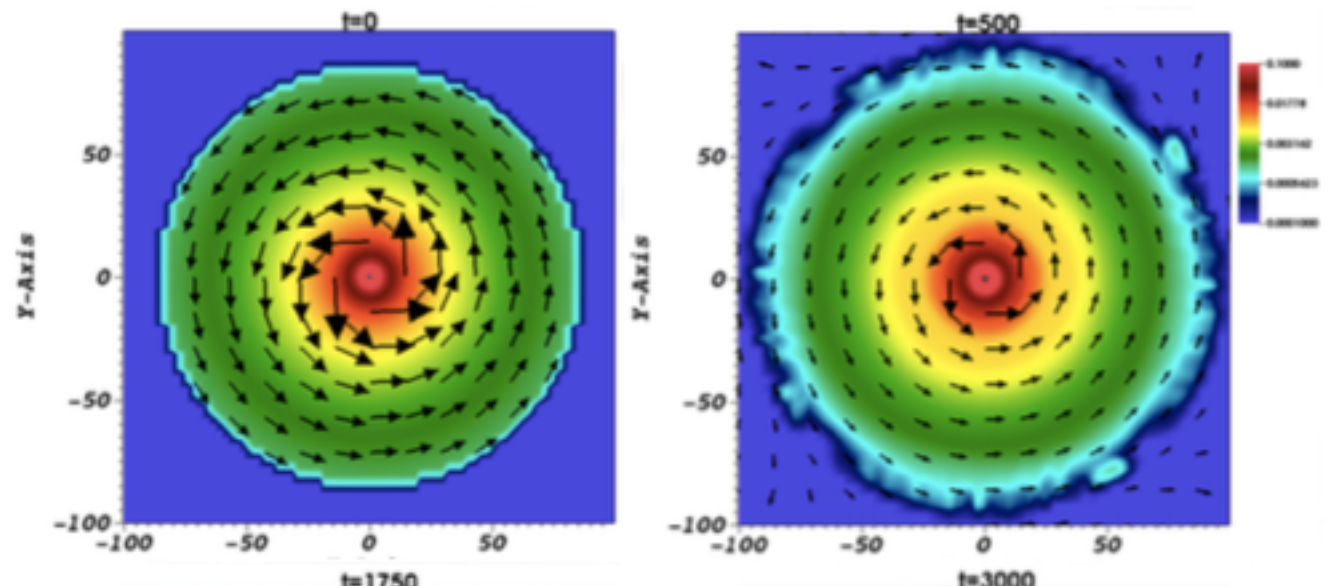
Run	$\eta$	$q$	$h$	$D$	$\beta$	$L_1^p [x, y, z]$
Single star with jet launching disk						
s case1	0.03	-	-	-	20	-
s case2	0.03 for $z < 10$	-	-	-	20	-
s case3	$3h_2 V_A$	-	-	-	20	-
s case4	$0.03h_3$	-	-	-	20	-
s case5	$0.03h_2$	-	-	-	20	-
s case6	0.03 for $z < 5$	-	-	-	20	-
Binary system with jet launching disk around primary						
b case1	0.03 for $z < 10$	2	60	300	20	(130, 0, 26)
b case2	0.03	1	60	200	20	(100, 0, 30)
b case3	0.01	2	60	300	20	(130, 0, 26)
b case4	0.03 for $z < 10$	2	60	200	20	(130, 0, 26)

初期回転 初期回転

$$v_\phi(r) = \sqrt{\frac{GM}{r}} \begin{cases} 0, & \text{for } 0 < r < r_0 \\ \sqrt{1 - 5\epsilon^2}, & \text{for } r_0 < r < r_i \\ \sqrt{1 - 2.5\epsilon^2}, & \text{for } r_i < r < r_{\max} \\ 0, & \text{for } r > r_{\max} \end{cases}$$

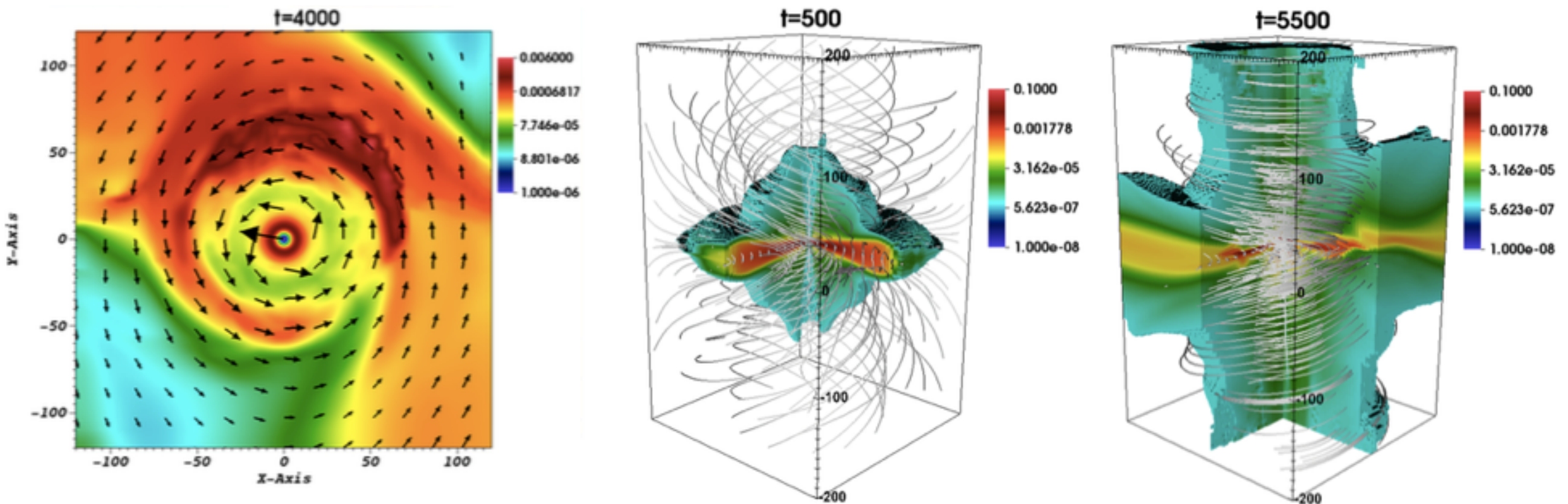
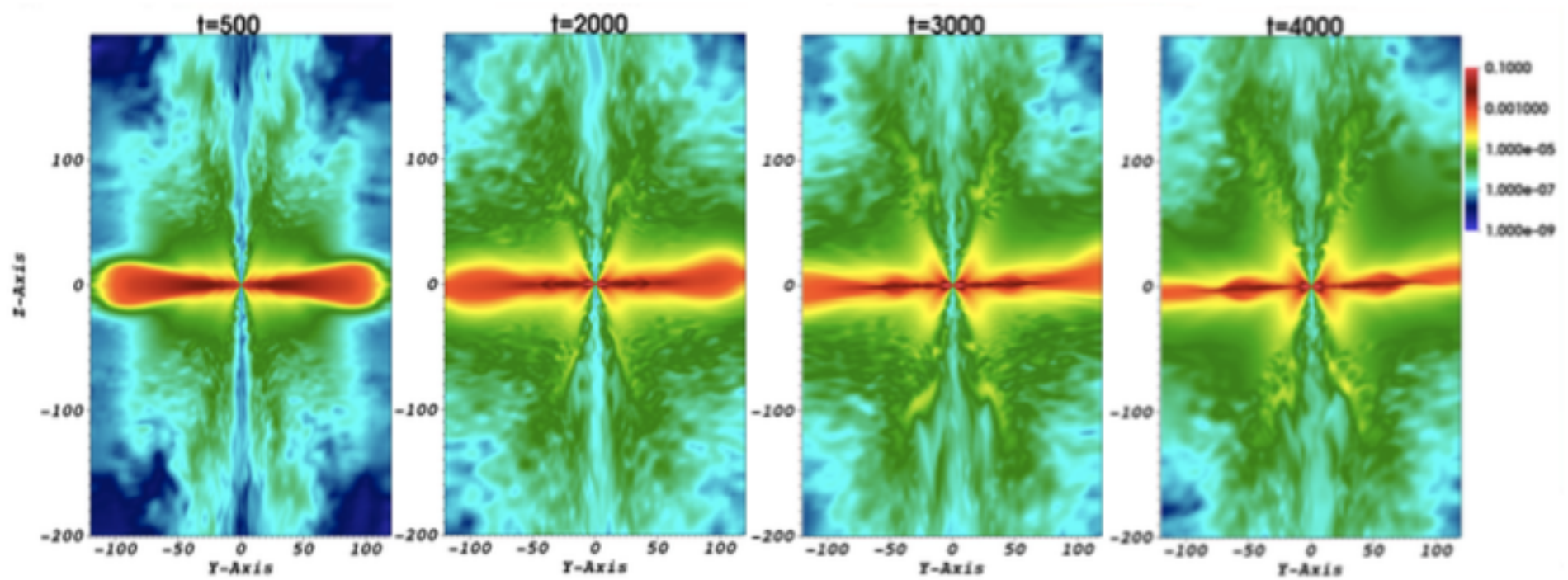


单独星の場合



$\Delta x = \Delta y = \Delta z = 0.05$   
 $-5 < x, y, z < 5$   
+stretched grid

# 連星の場合



Disk

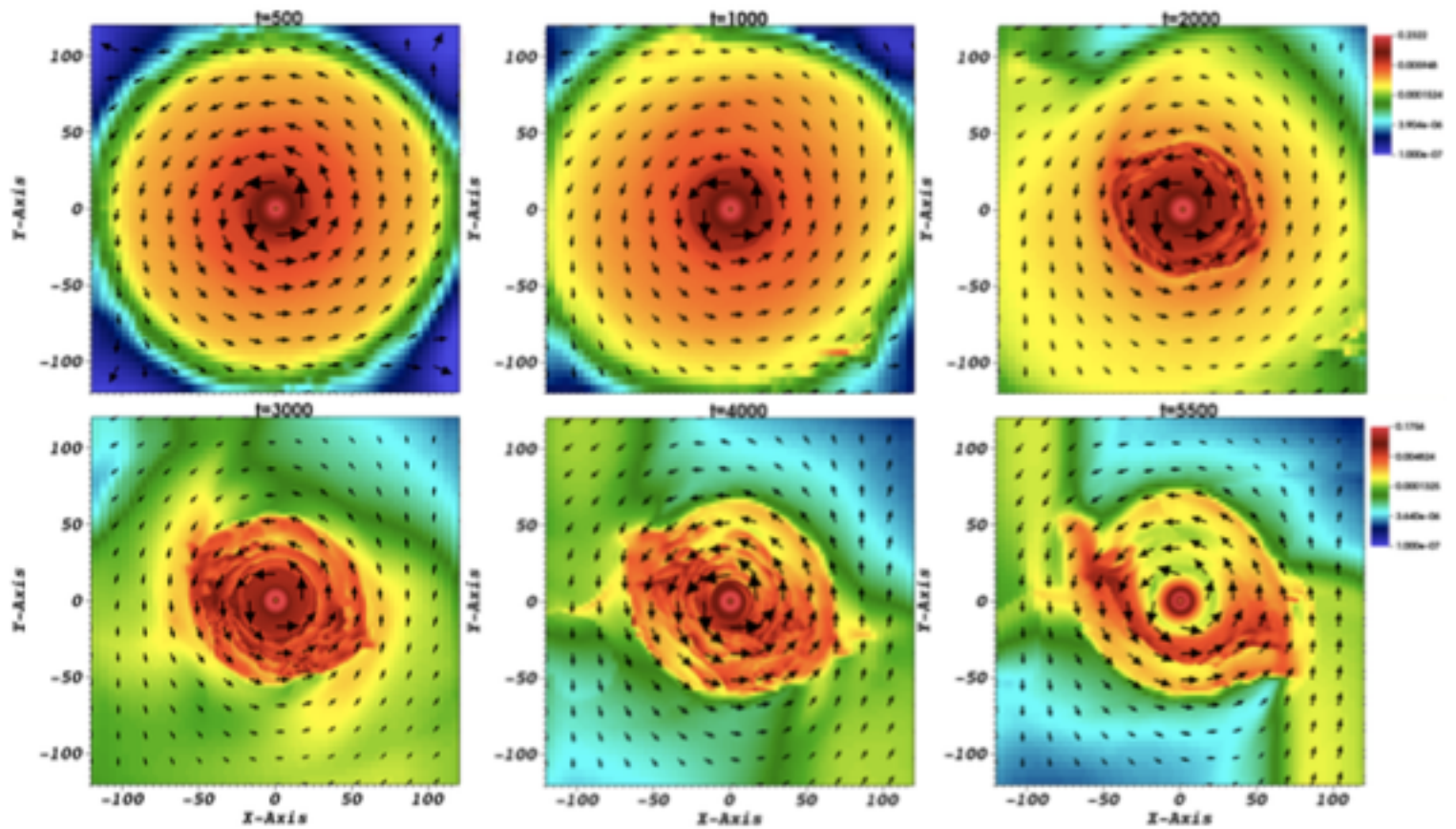


**Figure 12.** Non-axisymmetric evolution of the disk. Shown are the two dimensional slices done for the mass density distribution, in the  $x - y$  plane for bcase2 at different dynamical times. The arrows indicate to the velocity vectors of the disk.

Jet  
(precession)

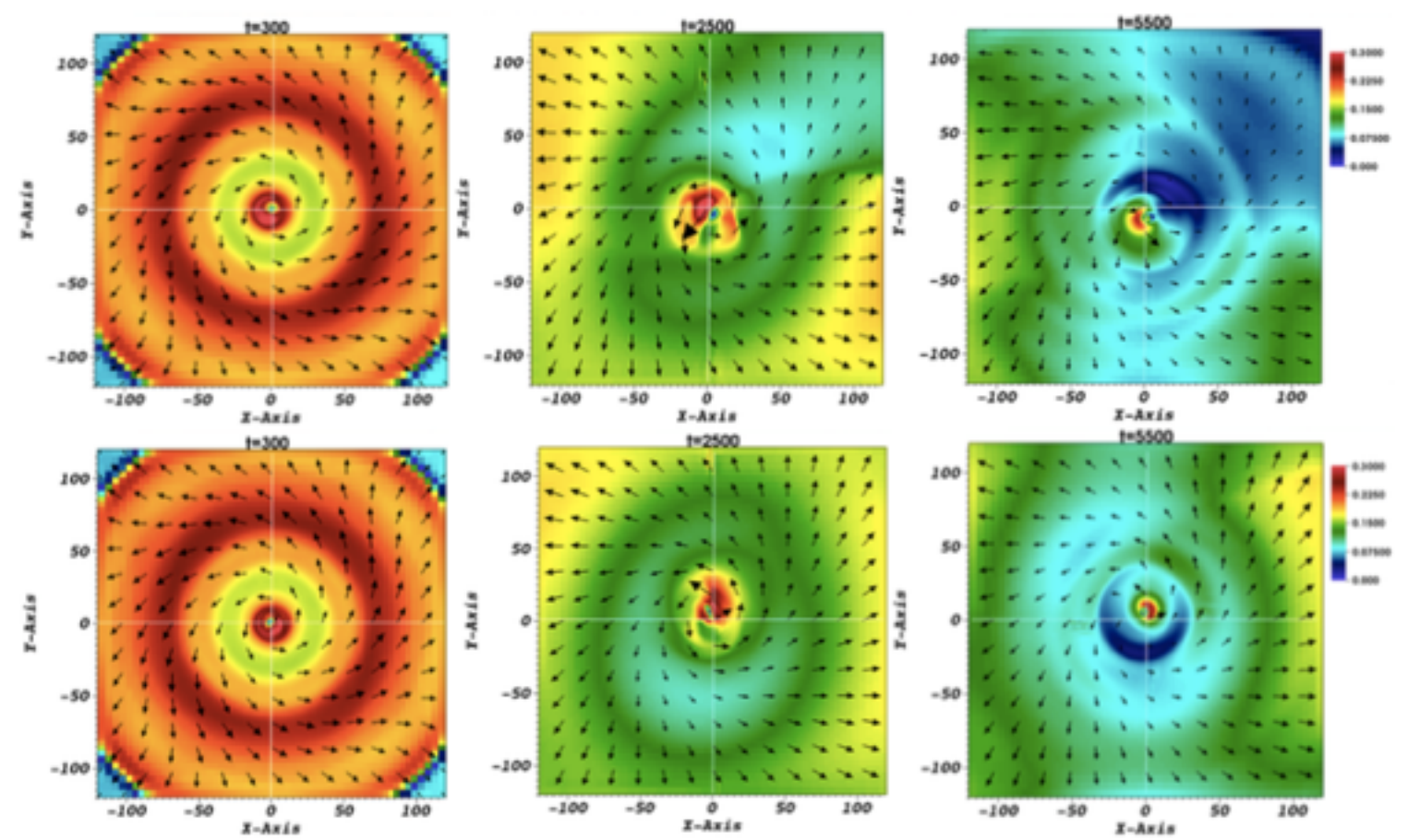
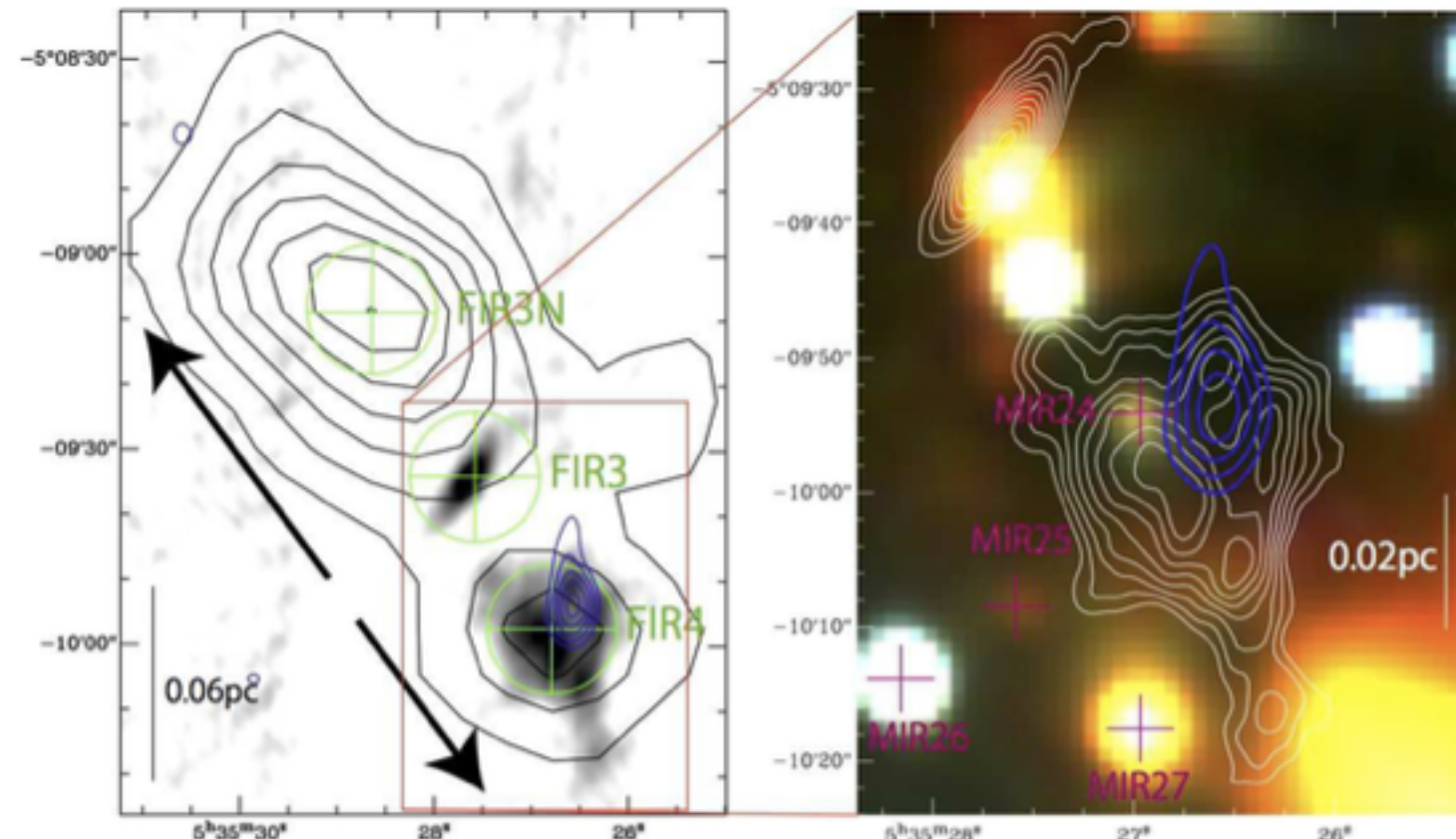


**Figure 13.** Indication of jet precession. Shown is the cross section of the projected velocity (color-coded) in the  $x-y$  plane at  $z = 140$  (top, jet) and at  $z = -140$  (bottom, counter jet) for the simulation bcase2 at different times. The white lines indicate the grid center, thus the initial disk/jet rotational axis. The arrows indicate the velocity vector field.

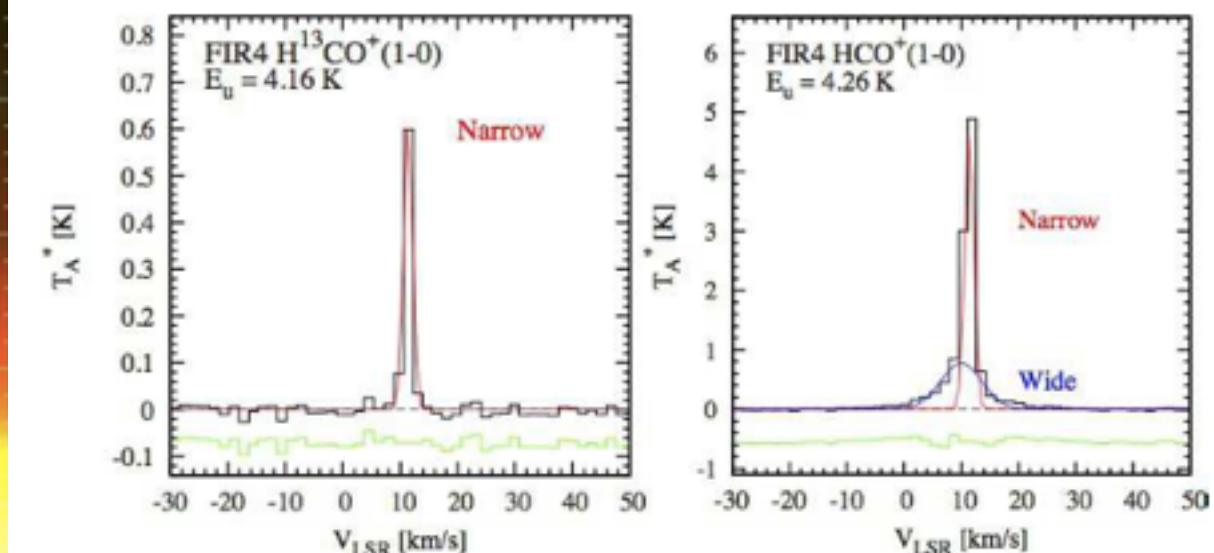
# Spectral-Line Survey at Millimeter and Submillimeter Wavelengths toward an Outflow-Shocked Region, OMC 2-FIR 4

Y. Shimajiri *et al.* ApJS

82-106 GHz, 335-355 GHz 120 lines, 20 molecules

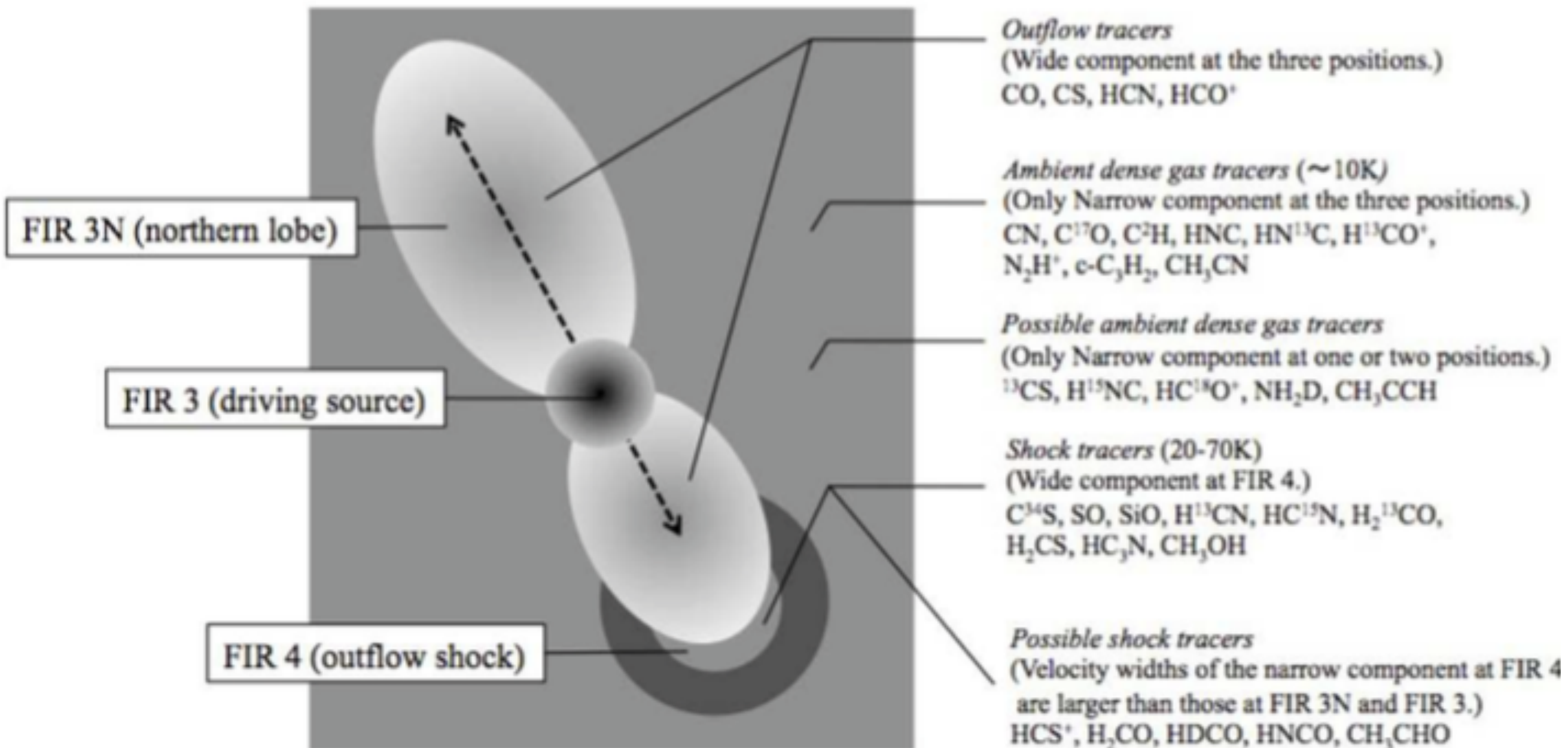


two types



wide/narrow  $3 \text{ km s}^{-1}$

# Fig. 8 Summary

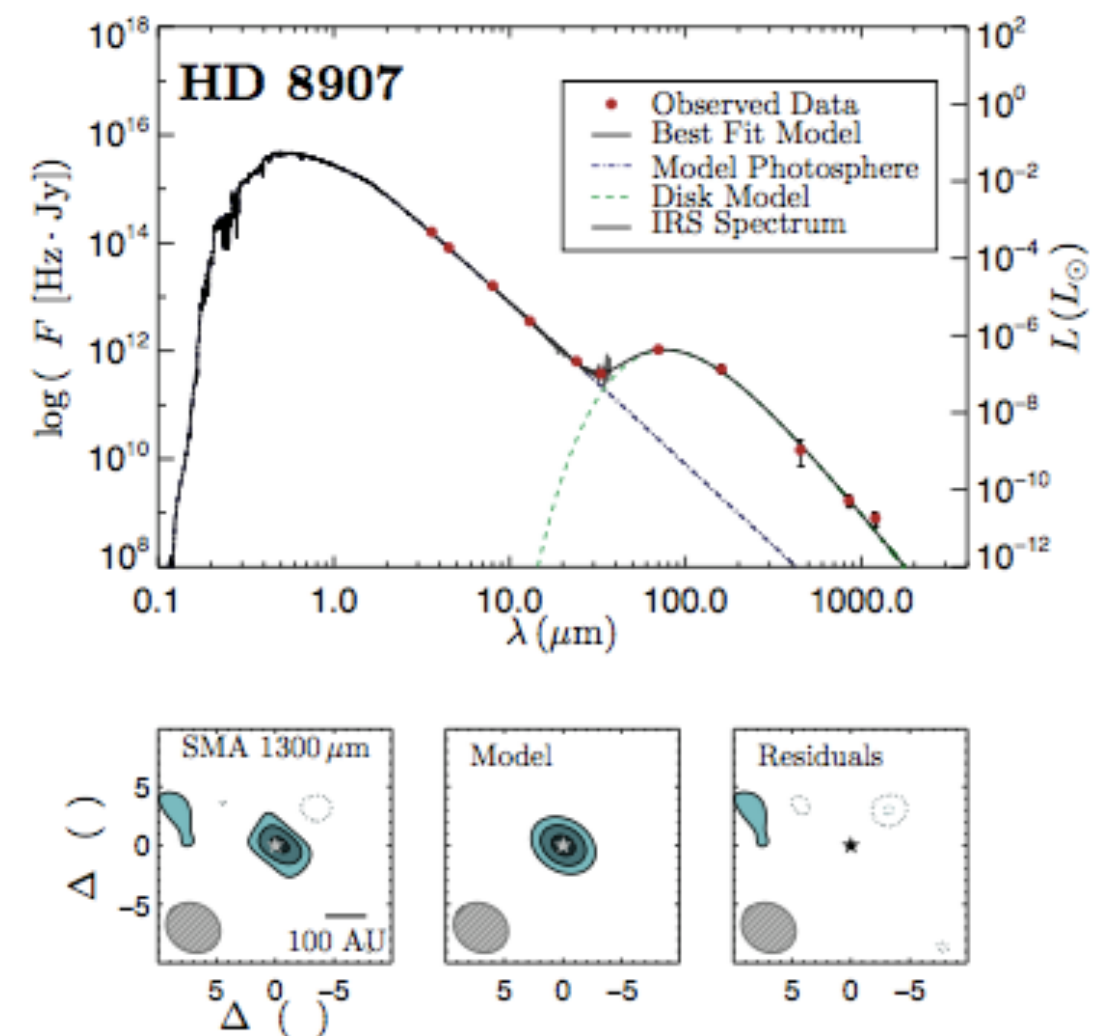
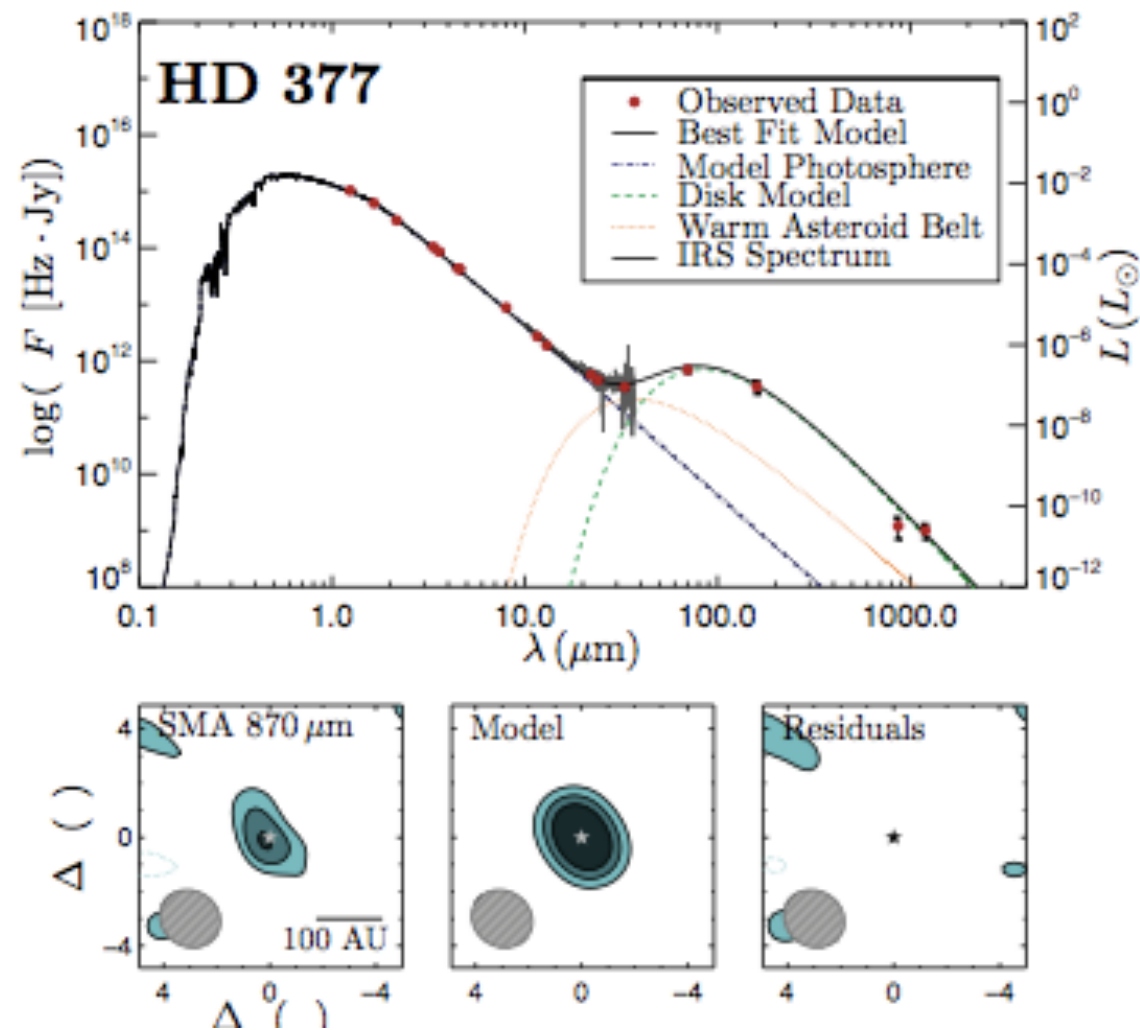


Species	FIR 3N		FIR 3		FIR 4		Physical environment
	Narrow	Wide	Narrow	Wide	Narrow	Wide	
CN	o	...	o	...	o	...	ambient dense gas
C <sup>17</sup> O	o	...	o	...	o	...	ambient dense gas
C <sub>2</sub> H	o	...	o	...	o	...	ambient dense gas
HNC	o	...	o	...	o	...	ambient dense gas
HN <sup>13</sup> C	o	...	o	...	o	...	ambient dense gas
H <sup>13</sup> CO <sup>+</sup>	o	...	o	...	o	...	ambient dense gas
N <sub>2</sub> H <sup>+</sup>	o	...	o	...	o	...	ambient dense gas
c-C <sub>3</sub> H <sub>2</sub>	o	...	o	...	o	...	ambient dense gas
CH <sub>3</sub> CN	o	...	o	...	o	...	ambient dense gas
<sup>13</sup> CS	...	...	o	...	o	...	(possible) ambient dense gas
H <sup>15</sup> NC	o	...	...	...	o	...	(possible) ambient dense gas
HC <sup>18</sup> O <sup>+</sup>	...	...	o	...	...	...	(possible) ambient dense gas
NH <sub>2</sub> D	...	...	...	...	o	...	(possible) ambient dense gas
CH <sub>3</sub> CCH	...	...	o	...	o	...	(possible) ambient dense gas
CO	o	o	o	o	o	o	molecular outflow
CS	o	o	o	o	o	o	molecular outflow
HCN	o	o	o	o	o	o	molecular outflow
HCO <sup>+</sup>	o	o	o	o	o	o	molecular outflow
C <sup>34</sup> S	...	...	o	...	o	o	outflow shock
SO	o	...	o	o	o	o	outflow shock
SiO	...	...	...	...	o	o	outflow shock
H <sup>13</sup> CN	o	...	o	...	o	o	outflow shock
HC <sup>15</sup> N	...	...	o	...	o	o	outflow shock
H <sub>2</sub> <sup>13</sup> CO	o	...	o	...	o	o	outflow shock
H <sub>2</sub> CS	o	...	•	...	o	o	outflow shock
HC <sub>3</sub> N	o	...	o	...	o	o	outflow shock
CH <sub>3</sub> OH	o	...	•	...	o	o	outflow shock
HCS <sup>+</sup>	...	...	...	...	•	...	(possible) outflow shock
H <sub>2</sub> CO	...	...	...	...	•	...	(possible) outflow shock
HDCO	...	...	•	...	•	...	(possible) outflow shock or (possible) molecular outflow <sup>a</sup>
HNCO	...	...	o	...	•	...	(possible) outflow shock
CH <sub>3</sub> CHO	...	...	o	...	•	...	(possible) outflow shock

# RESOLVED MILLIMETER-WAVELENGTH OBSERVATIONS OF DEBRIS DISKS AROUND SOLAR-TYPE STARS

A. Steele *et al.* ApJ

Spitzer survey にもとづく SMA, CARMA, ALMA 観測



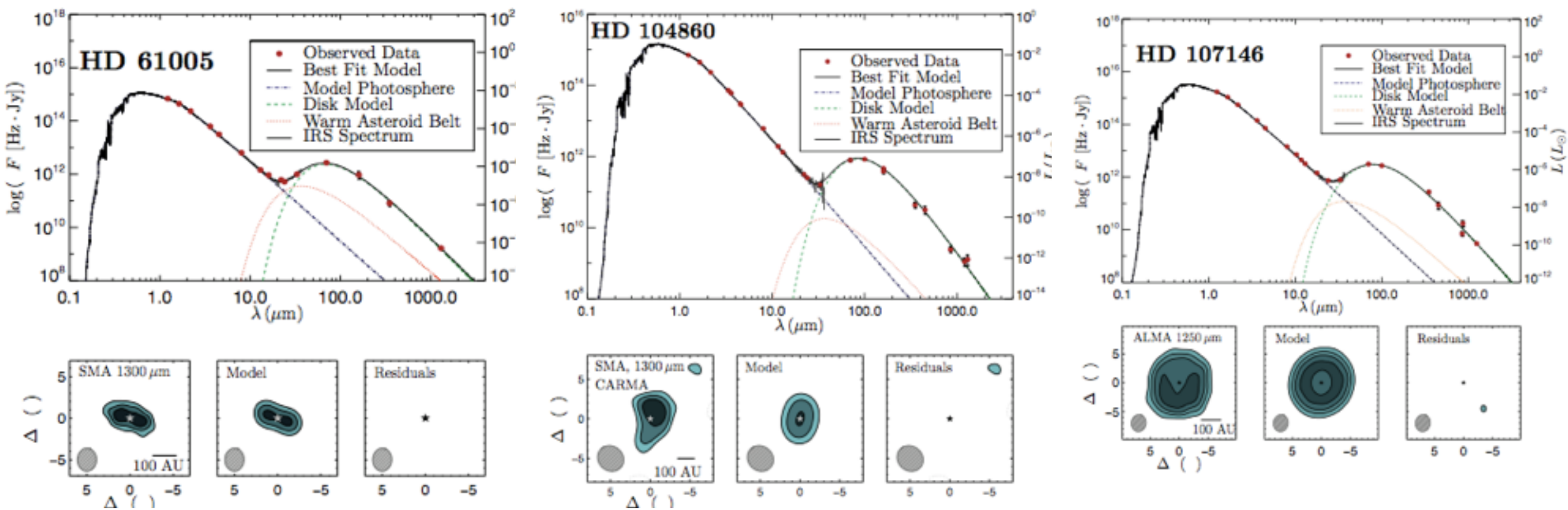


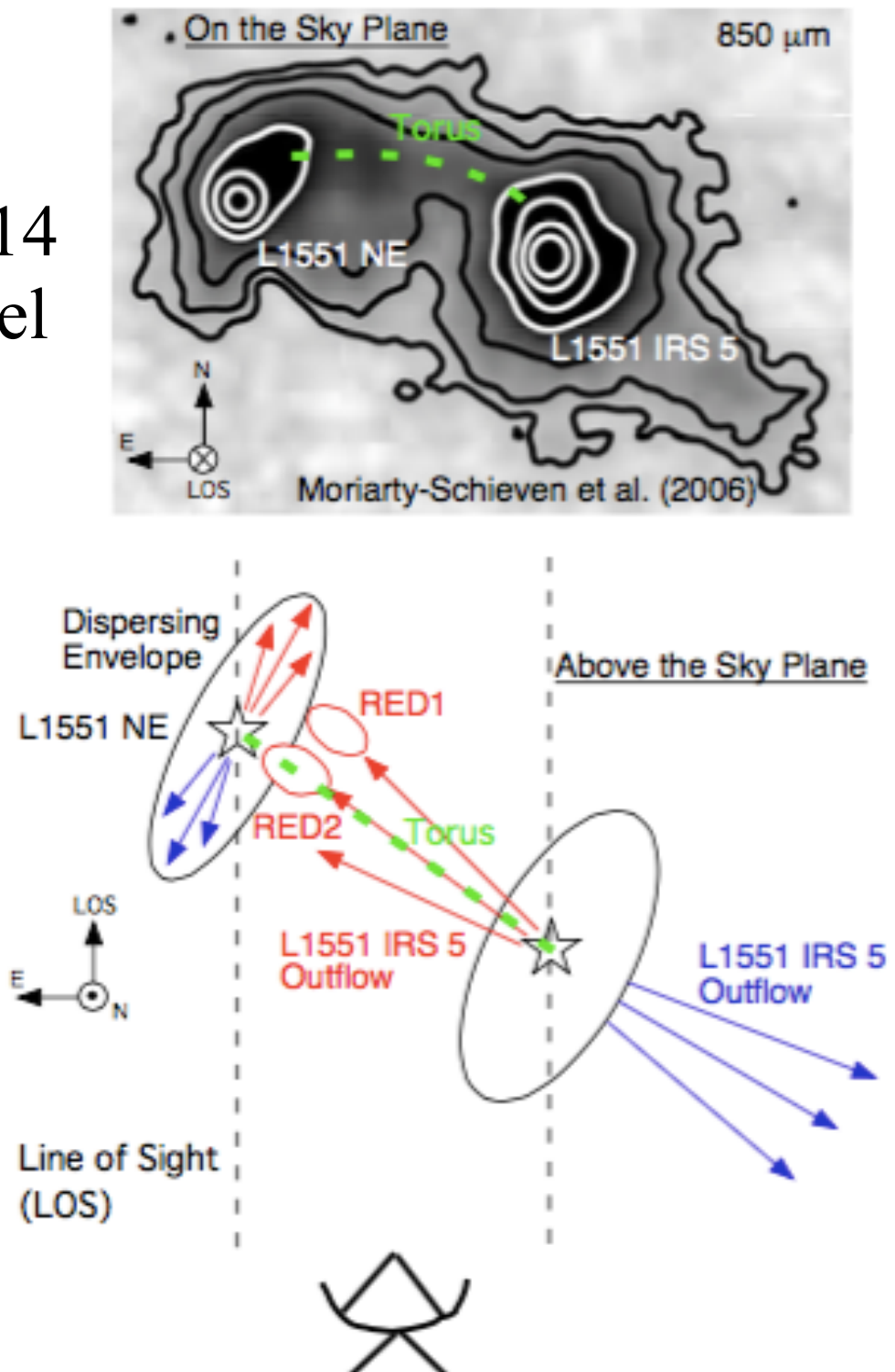
TABLE 7  
THE BEST-FIT PARAMETERS FOR ALL DISKS

Source	$a(\mu\text{m})$	$M_D(10^{-3}M_\oplus)$	$M_B(10^{-5}M_\oplus)$	$\beta$	$R_{\text{in}}(\text{AU})$	$R_{\text{in,avg}}$	$\Delta R$ (AU)	$p$	Total $\chi^2$	$\chi^2_{\text{Red}}$	
HD 377	19.8 $33.5^{+39}_{-16}$	5.57 $8.38^{+4.64}_{-2.99}$		3.26 $3.13^{+0.33}_{-0.36}$	0.76 $0.96^{+0.51}_{-0.21}$	31 $30.1^{+8.4}_{-6.3}$	47	32 $32.9^{+16}_{-18}$	-	269023.48	1.40
HD 8907	24.9 $15.4^{+13}_{-7.6}$	4.93 $4.49^{+2.05}_{-1.57}$	$2.68 \times 10^{-5}$ <sup>(a)</sup>	1.13 $1.05^{+0.16}_{-0.15}$	28 $36.4^{+19}_{-10}$	54	52 $53.2^{+31}_{-32}$	-	357244.56	1.89	
HD 61005	1.17 $1.03^{+0.46}_{-0.54}$	0.854 $0.71^{+0.54}_{-0.43}$	2.99 $4.26^{+0.17}_{-1.3}$	0.46 $0.43 \pm 0.08$	69.4 $70.9^{+3.0}_{-4.7}$	71	- <sup>b</sup> - <sup>b</sup>	-	456165.08	1.85	
HD 104860	4.27 $4.00^{+1.63}_{-1.12}$	7.20 $6.87^{+2.42}_{-2.17}$	1.68 $0.193^{+2.3}_{-0.019}$	0.75 $0.74 \pm 0.08$	57 $63.3^{+24}_{-11}$	110	108 $87.9^{+24}_{-43}$	-	377760.86	2.38	
HD 107146	4.71 $5.05^{+0.81}_{-0.78}$	8.85 $9.51^{+1.27}_{-1.95}$	0.197 $0.241^{+0.069}_{-0.049}$	0.74 $0.75^{+0.02}_{-0.05}$	29.4 $30.8^{+2.0}_{-1.7}$	94	129 $129^{+2.1}_{-1.9}$	-0.57 $-0.50^{+0.08}_{-0.07}$	490862.26	1.18	

dust は blowout されるより少し大きい  
破碎により作られた

# Dispersing Envelope around the Keplerian Circumbinary Disk in L1551 NE and its Implications for the Binary Growth

Fig. 14  
model



ASTE+SMA

Takakuwa *et al.* ApJ

Fig. 2 ASTE integrated intensity

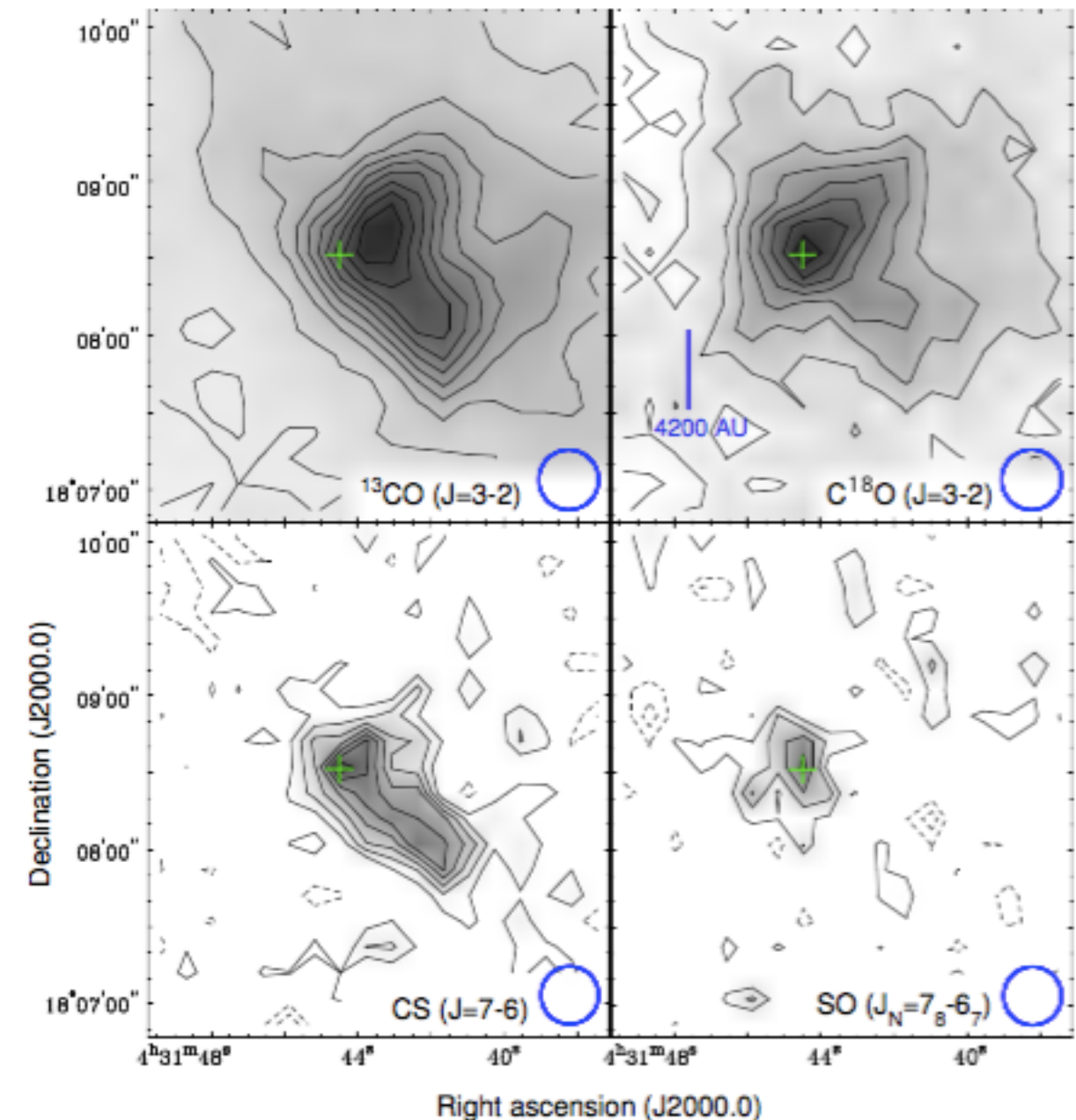


Fig. 6

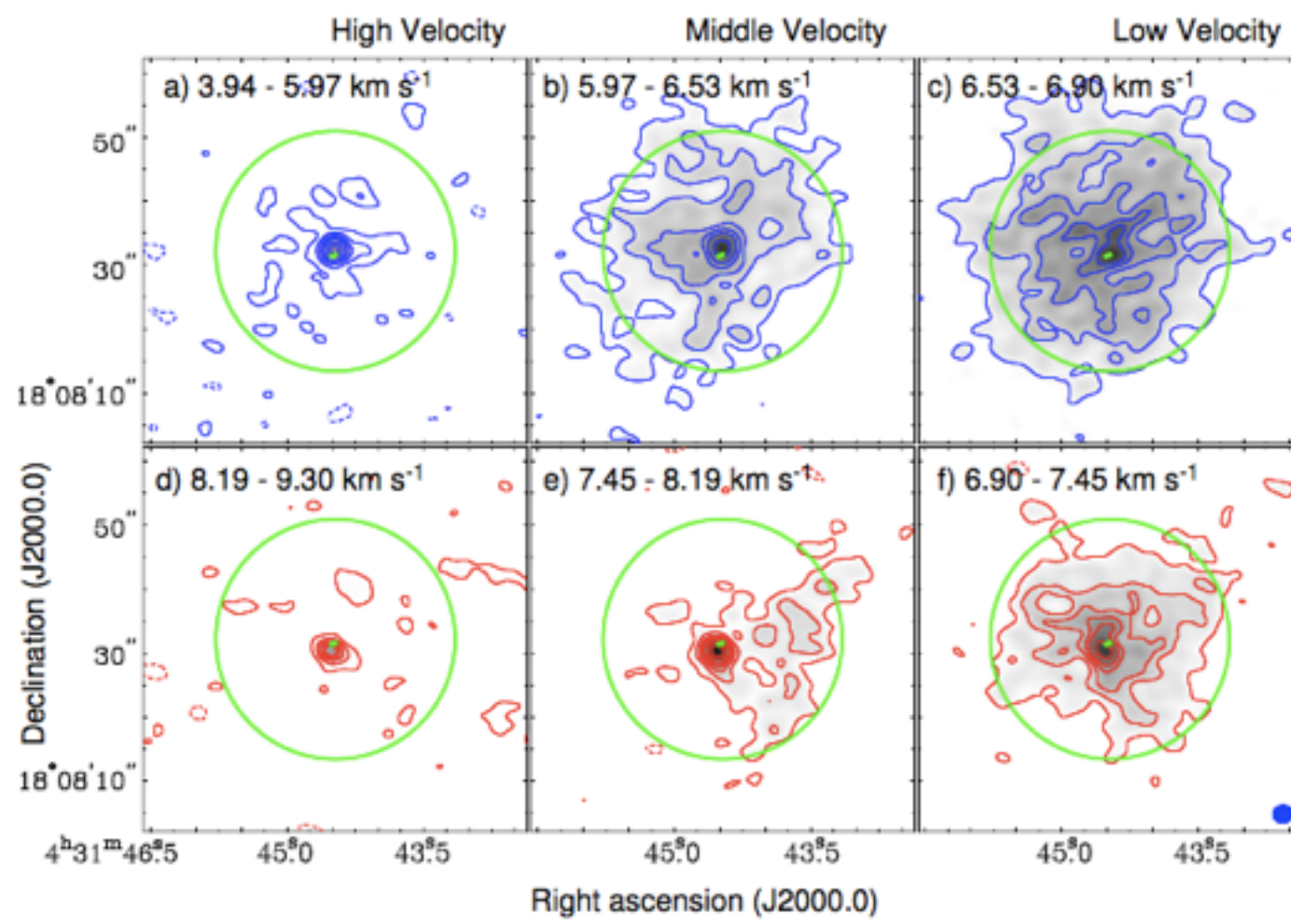
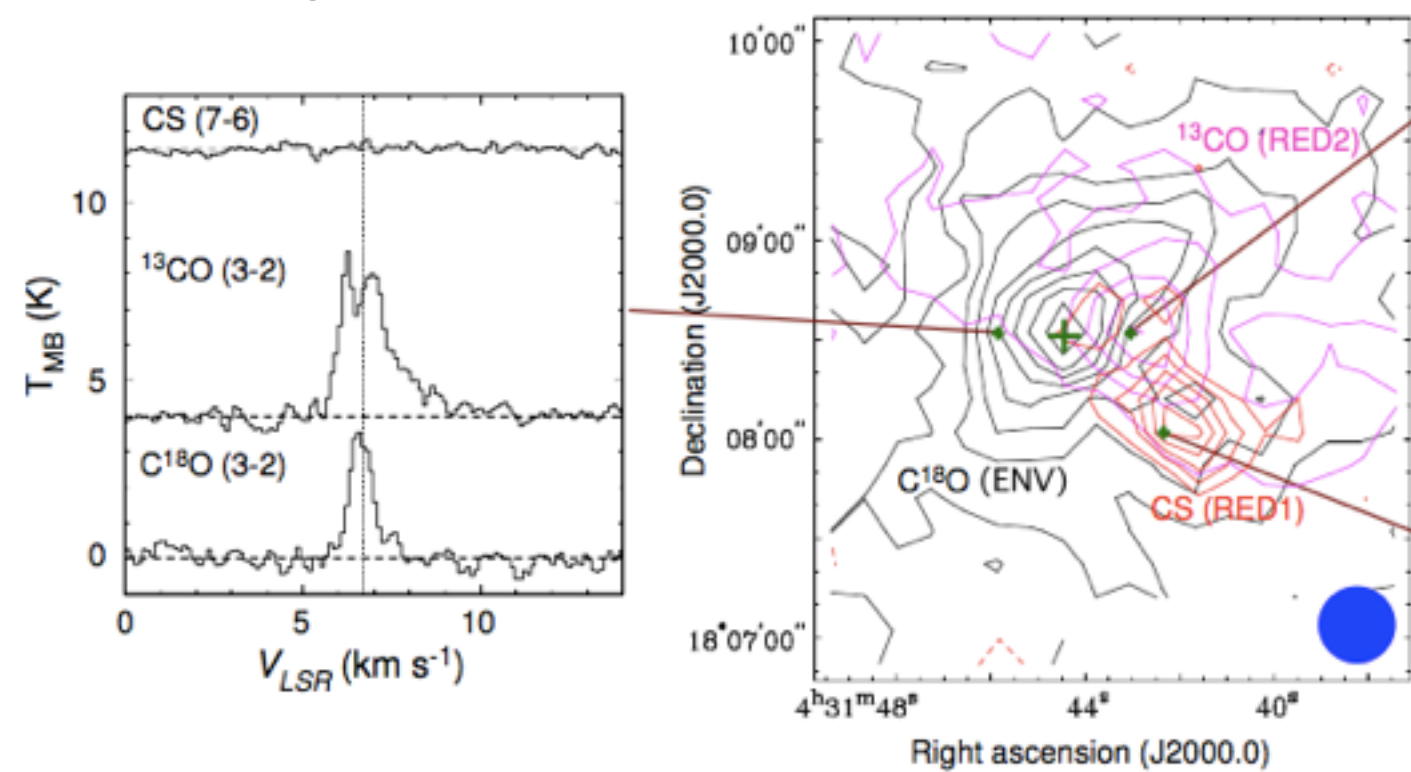


Fig. 11

## Summary

1. C18O Wide (Circum Binary D.) + Narrow (Extended Env.)
2. Dispersing Envelope + Outflow from L1551 IRS5
3. CBD  $\sim$  300 AU + Infalling Env.  $\sim$  700 AU
4. L1551 IRS5 からのOutflow は力学的なImpact
5. L1551 NEの質量と質量比は現在の値  $\sim 0.8 M_{\odot}$ ,  $q \sim 0.19$   
が最終値に近い